Digital Microfluidic Biochips: A Vision for Functional Diversity and More than Moore

Tsung-Yi Ho*, Jun Zeng†, and Krishnendu Chakrabarty‡
*Department of CSIE, National Cheng Kung University, Tainan, Taiwan
†Hewlett-Packard Laboratories, Hewlett-Packard Co., Palo Alto, CA
‡Department of ECE, Duke University, Durham, NC

Abstract

Advances in droplet-based digital microfluidics have led to the emergence of biochips for automating laboratory procedures in biochemistry and molecular biology. These devices enable the precise control of microliter of nanoliter volumes of biochemical samples and reagents. They combine electronics with biology, and integrate various bioassay operations, such as sample preparation, analysis, separation, and detection. Compared to conventional laboratory procedures, which are cumbersome and expensive, miniaturized digital microfluidic biochips (DMFBs) offer the advantages of higher sensitivity, lower cost, system integration, and less likelihood of human error. This tutorial paper provides an overview of DMFBs and describes emerging computer-aided design (CAD) tools for the automated synthesis and optimization of biochips, from physical modeling to fluidic-level synthesis and then to chip-level design. By efficiently utilizing the electronic design automation (EDA) technique on emerging CAD tools, users can concentrate on the development of nanoscale bioassays, leaving chip optimization and implementation details to design-automation tools.

1. Introduction

Digital microfluidic biochip (DMFB) is an emerging technology that aims to miniaturize and integrate droplet-based, functions on a chip. By manipulating droplets with microvolumes or nano-volumes, the DMFB provides higher sensitivity and less human errors compare to benchtop procedures. Furthermore, the miniaturization and automation offer less reagent consumption and more flexible control [1], [2]. Due to these advantages, DMFBs are expected to revolutionize many biological processes, especially for the immediate point-of-care diagnosis of diseases.

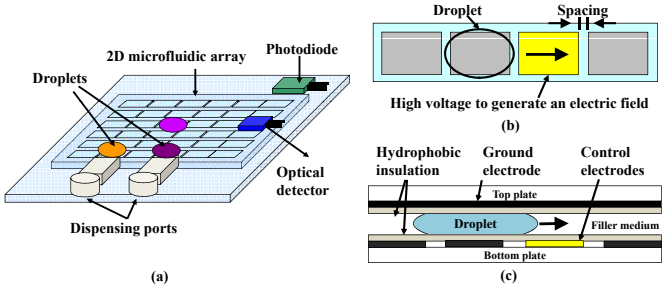

Figure 1. A digital microfluidic biochip (DMFB). (a) Schematic view of a DMFB. (b) Top view of the 2D microfluidic array. (c) Side view of the 2D microfluidic array.

Figure 1(a) shows the schematic view of a DMFB. A DMFB contains three components, the 2D microfluidic array, the dispensing ports/reservoirs, and the optical detectors. The 2D microfluidic array contains a set of basic cells which consist of two parallel glass plates (see Figure 1(b)(c)). The bottom plate contains a patterned array of individually controllable electrodes, and the top plate is coated with a continuous ground electrode. The filler medium, such as silicone oil, are sandwiched between the plates. By independently controlling the voltage of electrodes, droplets can be moved along this line of electrodes due to the principle of electrowetting-on-dielectric (EWOD) [3], [4]. Therefore, many fluidic operations such as mixing and dilution can be performed anywhere in the 2D array within different time intervals. This characteristic is also referred to as the *reconfigurability* [1]. Besides the 2D microfluidic array, there are on-chip reservoirs, dispensing ports, and optical detectors. The dispensing ports are responsible for droplet generation while the optical detectors are used for droplet detection.

Recently, many on-chip laboratory procedures such as immunoassay, real-time DNA sequencing, and protein crystallization have all been successfully demonstrated on DMFBs. Continuing growth of applications in this emerging field complicates the chip/system integration and design complexity. As the number and size of DMFBs is expected to ramp up in the coming years, there is an urgent need for high-quality software tools to assist in the design automations, especially for physical modeling, fluidic-level synthesis, and chip-level design [2], [5], [6], [7].

This tutorial paper is focus on emerging computer-aided design (CAD) tools for the automated synthesis and optimization of DMFBs, The basic architecture and physical principles underlying droplet movement are explained. Recent advances in modeling, simulation, resource binding, operation scheduling, module placement, droplet routing, chip-level design, and testing are also introduced. These CAD techniques allow biochip users to concentrate on the development of nanoscale bioassays, leaving chip optimization and implementation details to design-automation tools.

It is expected that an automated design flow will transform the biochip research and use, in the same way as design automation revolutionized the IC design in 1980s and 1990s. This approach is therefore especially aligned with the vision of functional diversification and *More than Moore* as articulated in the International Technology Roadmap for Semiconductors 2007, which highlights Medical as being a System Driver for the future. Biochip users will adapt more easily to emerging technology if appropriate design methods/tools and in-system automation methods are available.

The rest of this paper is organized as follows. Section 2 describes the physics of droplets, flow modeling, and device simulation methods. Section 3 presents synthesis techniques, including recent results on scheduling, resource binding, and droplet routing. Section 4 is focused on automated chip design, especially optimization techniques for pin-limited biochips. Finally, Section 5 examines defects, fault models. and testing techniques.

978-1-4244-8192-7/10/$26.00 ©2010 IEEE

2. Device Physics, Modeling, and Simulation

Microfluidics research is witnessing a paradigm shift from the continuous-flow based architecture to the droplet based architecture, in particular, the digital microfluidics. Using droplets as "chemical processing plants" has operational benefits in addition to the architectural advantages mentioned in previous sections.

The larger surface-to-volume ratio and flow circulation within a droplet provide efficient mixing and thermal dissipation, and enable shorter reaction times. Each droplet is an independent reactor; it compartmentalizes sample species, eliminating the issues associated with Taylor-Aris dispersion that has been detrimental for continuous-flow based architecture.

From the architecture perspective, digital microfluidics exploits the "architectural dynamics" to the fullest extent: it uses electrode array of repeating pattern to address droplets, and the electrodes can be dynamically grouped to deliver certain functions and then disbanded afterwards and released to the shared resource pool; it enables dynamic re-configurability such that the routing of droplets is not statically planned beforehand rather dynamically created on the fly to enable the shortest response to exception. Digital microfluidics minimizes the complexity and specificity at the hardware level, and leaves all the decision-making (e.g., resource allocation, resource-task binding, task routing) to the runtime software. This enables digital microfluidics to be potentially a general-purpose platform; users can implement their own specific applications by programming their own operations instruction software onto the same hardware infrastructure - On this point, one may be able to draw a clear parallel with computing architecture evolution over past few decades.

With digital microfluidics, complex procedures are built up through combining and reusing a finite set of basic instructions including droplet generation, droplet translocation, droplet fusion, and droplet fission. Hydrodynamic forces generated by diverse actuation methods have been exploited to accomplish this set of operations.

It is commonly recognized that the first systematic scientific study of droplets was Savart's report on drop breakup mechanism in 1833. Rayleigh's work on interfacial stability analysis in 1879 provided the theoretical foundation for the discoveries of droplet physics continuing as recent as 1970s. While theoretical works have provided qualitative understanding of many interfacial phenomena, the quantitative prediction and analysis of droplet dynamics is still an active research field relying on modeling and numerical simulation techniques.

The continuum assumption holds for microfluidics [9]. Excluding a few exceptions (e.g., piezoelectric inkjet), the compressibility of the operating liquid can be considered effectively zero. The Navier-Stokes equations thus can be applied to govern the hydrodynamics of both the droplets and the continuous phase. Interfacial stress balance is preserved at the interface between a droplet and the continuous phase [10]. In the cases that the droplet is in contact with a solid surface, the interaction among molecules of the three phases (droplet, the continuous phase, and the solid) leads to a net force of attraction (wetting) or repulsion (non-wetting). This force, the wetting force, is a line force density acting on the tri-phase contact line, and is in plane with the solid surface, perpendicular to the tri-phase contact line, and points away from the droplet.

The governing equations described above unveil several possible knobs for droplet manipulation. Due to droplets' large surface-to-volume ratio, the forces (or moments) proportional to droplet volume usually are less effective comparing to forces acting on the droplet surface and/or on the tri-phase contact line. Net surface or wetting forces can be achieved through creating non-uniform distribution of surface tension, contact angle or surface pressure. Below are a few practical examples: (1) utilizing the thermal Marangoni effect [11], either through an array of embedded microheaters [12] or laser heating [13] temperature gradients thus the net surface force can be established and modulated; (2) Non-uniform distribution of surface pressure can also result in a net surface force (e.g., T-channel [14]); (3) Magnetic field can be used for droplet manipulation [15]; and (4) The use of the electric field to carry out on-chip droplet operation is largely based upon either dielectrophoresis [16] or electrowetting on dielectric (EWOD) [17] operating principles, that is, the discontinuity of the electrical properties of the media (droplet, the continuous phase, and the solid) at the droplet surface and/or the tri-phase contact line gives rise to a significant and highly controllable surface and/or wetting forces. Digital microfluidics systems based on EWOD has been developed furthest in terms of demonstrating on-chip applications that are clinically relevant [18].

Generating droplets is one of the most challenging on-chip droplet operations. It requires injecting significant amount of work to compensate the increase of the interfacial energy due to the enlarged total interfacial area. In addition, droplet breakup is an inherently stochastic process (Rayleigh instability). The capability of producing a net force that is significant compared to the surface tension force is the key to accomplish the on-chip liquid disintegration operations in a controlled fashion including droplet generation and droplet fission. On this, actuation technologies utilize wetting forces (e.g., EWOD) holds advantage.

Since the inception of microfluidics, the electric force has been exploited as one of the leading mechanisms for driving and controlling the movement of operating fluid and charged suspensions. The electric force has an intrinsic advantage in miniaturized devices. Because the electrodes are placed cross a small distance, from sub-millimeter to a few microns, a very high electric field, order of MV/m, is rather easy to obtain. In addition, the electric force can be highly localized force, with its strength rapidly decaying moving away from the peak. This makes the electric force an ideal candidate for spatial precision control. The geometry and placement of the electrodes can be used to design electric fields of varying distributions, which can be readily realized by MEMS fabrication methods. Electric control also possesses advantages in system integration and reliability. For instance, there are no mechanical moving parts, and the system can be directly controlled through software.

In most electrically controlled digital microfluidics platforms, droplets, the continuous phase and contacting solid phase possess different electric properties. This results in the discontinuity of the electric field intensity at the material boundaries (e.g., the droplet surface and the tri-phase contact line), which in turn results in gradient of the electrostatic energy thus gives rise of hydrodynamic forces of electric origin. During this transient conductive phase, the free floating charges within the droplets will accumulate at the droplet surface to support the electric field discontinuity at the material boundaries. This surface charge density is directly linked with the applied voltage and the EWOD force magnitude. Consequently EWOD is also referred to as a charge-controlled method.

The underlying mechanisms of most interfacial phenomena were qualitatively understood by 1970s. However, to this day quantitative analysis and descriptions of many systems are still lacking. Modeling and numerical simulation approaches play a significant role in providing detailed quantification of the droplet dynamics. With the aid of the ever increasing computing power, numerical simulations are able to offer physical insights that are otherwise difficult to measure experimentally, provide evaluations of design performance and experimental strategies, and help to interpret experimental results.

One of the earliest works on numerical simulations of interfacial problems would be Birkhoff's work with Los Alamos Scientific Laboratory during 1950s. The unique challenge in simulating droplet dynamics is to model the evolution of

droplet surface and the topological change due to droplet breakup and/or droplet merge. There are two families of numerical schemes to describe the movement of the droplet surface. This Lagrangian approach provides sharp interface description; however, it faces insurmountable numerical challenge when the droplets undergo topological changes such as breakup and merge. The other approach, the Eulerian approach uses a function defined within a fixed numerical grid to describe the droplet surface. This approach captures the droplet surface by solving an additional transport equation therefore it is also referred to as front-capturing approach. Examples of this approach include Marker-And-Cell [19], Volume-of-Fluid [20], and Level-Set [21]. Because of the implicit nature of this family of interface-capturing schemes, complexities arise from interface reconstruction procedures. The advantage of the Eulerian approach is its capability of simulating topological changes of the droplet surface. A Lagrangian-Eulerian hybrid, the front-tracking method [22] was also developed. Its major drawback is the complexity of the associated interface reconstruction algorithms. The most recent addition is the lattice Boltzmann method [23], of which, the accuracy and efficiency, comparing to more conventional methods, are still in active debate. From the perspective of (pareto)-optimal balancing among accuracy, efficiency and practicality, the front-capturing methods are the favorite of the practitioners, in particular, volume-of-fluid and level-set. In fact, almost all the leading commercial simulation packages that can be applied to digital microfluidics simulations implement some variations of these two methods. The simulation examples shown below were generated using CoventorWare and FLOW-3D which implement volume-of-fluids methods.

As described above, modeling the topological change is one of the fundamental challenges for droplet dynamics simulations. Here we present such simulation example, that is, droplet fission process carried out by EWOD driven digital microfluidics [24]. An individually addressable electrode array can be used to program desired electric field such that a spatial variation of the EWOD force is generated at the tri-phase contact line. The net wetting force is then used to accomplish droplet generation, translocation, fission, and fusion. Figure 2(a) shows the device configuration. The electrodes are aligned along the x direction, and a droplet initially is centered in between two neighboring electrodes. Upon application of a voltage to all the electrodes, a spatial disparity of EWOD force is created. Figure 2(b) shows the simulation results. It can be observed that the contact angle at the tri-phase contact point closer to the electrodes (the vicinity of points W and E) is smaller than that at the tri-phase contact point further from the electrodes (the vicinity of points N and S). Consequently, the droplet is elongated in the x direction at both sides (along W-E plane), and simultaneously the y-z cross-section at the center of the droplet (on N-S plane) is reduced. Eventually the cross-section in the N-S plane reduces to a point and two droplets are created to conclude the fission process.

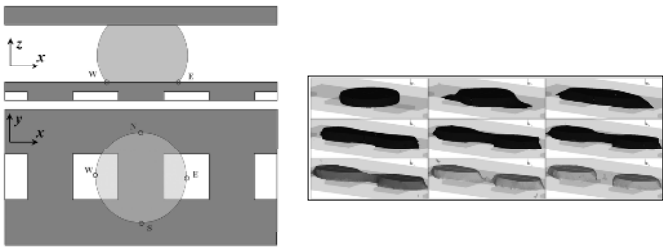

(a) (b)

Figure 2. Droplet fission on an EWOD-driven lab-on-a-chip [24].

3. Synthesis of DMFBs

Recent years have seen the interest in the automated design and synthesis of DMFBs [8]. For the purpose of efficiency, hierarchical and cell-based design methods in modern VLSI automations has been utilized to address the issue with *architectural-level* synthesis and *physical-level* synthesis, as shown in Figure 3. In this section, we introduce the two major synthesis models and examine a progression of related CAD problems.

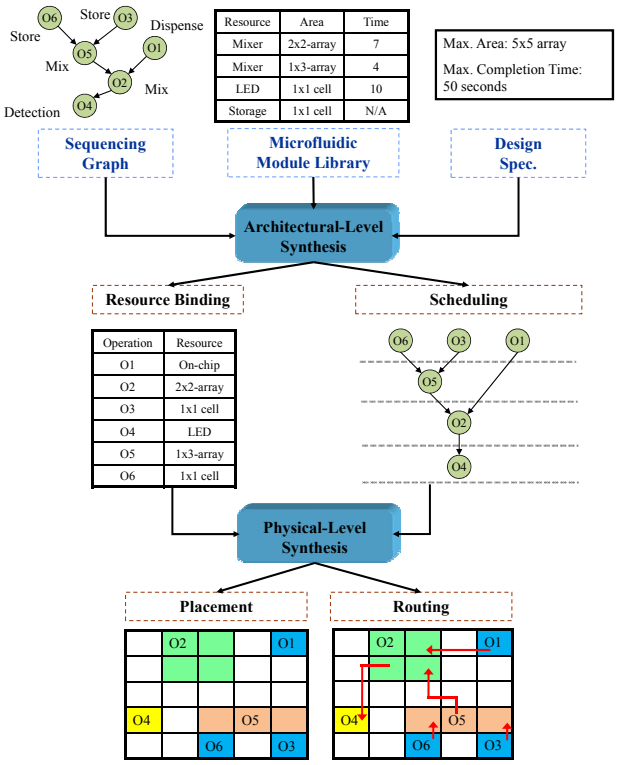

Figure 3. Synthesis of DMFBs.

3.1. Architectural-Level Synthesis

In designing DMFBs, a biochemical application is usually abstracted as a model of sequencing graph (see Figure 3). The sequencing graph is directed, acyclic and polar (i.e., there is a source node without predecessors and a sink node without successors). Each node represents a specific assay operation (e.g., mixing, generation, and detection), while a directed edge indicates the dependency between two operations.

In architectural-level synthesis, the major goal is to schedule the assay operations and bind them to a given number of resources (e.g., mixers or dilutions) so as to maximize the parallelism, thereby decreasing the execution time. This procedure is also referred to as *resource binding*, which determines the mapping from assay operations to available functional resources. Note that there may be several types of resources for any given assay operation. For example, a 1×4 mixer, a 3×2 mixer, and a 2×4 mixer can be used for a mixing operation but with different mixing times. In such case, a resource binding procedure must be applied to determine the selections. Once resource binding is carried out, the execution time for each assay operation can be easily found. In other words, scheduling of the start times and stop times of all assay operations is determined, subject to the precedence constraints

by the given sequencing graph. The resource binding and scheduling procedure can be illustrated in Figure 3.

The objective is to minimize the assay execution time, which is an essential requirement for many DMFB designs for the following reasons. First, since the biological samples are miniaturized to micro or nano scale, they are much sensitive to the environment and to the temperature variations. Unfortunately, it is difficult to maintain an optimal clinical or laboratory environment within a long execution time, and thus the integrity of assay results may be degraded. Besides, real-time response is also necessary for many safe-critical and point-of-care applications, such as surgery and neonatal clinical diagnostics. Especially the time-to-result effects in these applications are much more critical than others and must be avoided. Furthermore, decreasing the execution time also improves the operation and system reliability. Long assay execution time implies high actuation voltages needed to be maintained on the operational electrodes, which accelerate the insulator degradation and dielectric breakdown. These electric defects result in unexpected system behaviors and thus mislead assay outcomes. Therefore, the entire system reliability may be decreased [1], [8].

Several algorithms, such as tabu-search based synthesis [25] and ILP-based synthesis [26], are proposed to handle the basic architectural-level synthesis of DMFBs. In addition, for some complex biomedical applications such as clinical diagnostics, it is necessary to verify the correctness of on-chip fluidic operations. The status of an assay can be monitored by examining the volume of the droplet, sample concentration, or detector readout. If an error occurs during the execution of an assay, e.g., an unexpected volume of an intermediate droplet, the assay outcomes will be misleaded. Therefore, it is important to detect such errors as early as possible and re-execute the fluidic operations to obtain correct assay outcomes. Considering this issue, a control-path based design is recently integrated to the architectural-level synthesis of DMFBs [27]. In [27], they first calculate the possibilities of errors for each operation via an error-propagation estimates, and then insert a check point consisting of a storing operation and a error detection to the sequencing graph. A simulated-annealing (SA) method is also proposed to optimize the execution time used for error recovery.

3.2. Physical-Level Synthesis

After architectural-level synthesis, all the operations are bound to specific fluidic modules with totally minimized execution time. In physical-level synthesis, *placement* is first applied to determine the actual on-chip position of theses scheduled fluidic modules within different time intervals. Then, *droplet routing* constructs the connections between modules, and between modules and I/O ports (i.e., on-chip reservoirs). In the following subsections, we first introduce the placement problem and then discuss the droplet routing problem in the physical-level synthesis of DMFBs.

1) Placement. A key problem in the physical-level synthesis of DMFBs is the placement of fluidic modules such as different types of mixers and detection units. The major goal of the placement is to find the actual locations of different fluidic modules corresponding to different time intervals. Since DMFBs enable dynamic reconfiguration of the microfluidic array during run-time, they allow the placement of different modules on the same location during different time intervals [1], [28]. The physical placement problem of digital microfluidic biochips are closely related to the operations of dynamically reconfigurable FPGAs (DR-FPGAs), which have received much attention recently. However, there are some key differences. The programmability of DR-FPGAs is limited by the well-defined rules of interconnect and logic blocks. Interconnect cannot be used for storing information and logic blocks cannot be used for routing. By contrast, DMFBs offer significantly more dynamic reconfigurability. All the fluidic modules placed on the microfluidic array can be easily moved to anywhere on-chip locations, or be replaced with other fluidic modules in different time intervals.

The most important optimization objective of the placement problem is the minimization of chip area. Since solutions of the placement problem can provide the designers with guidelines on the chip size to be manufactured, area minimization frees up more unit cells for other fluidic functions such as sample preparation and collection. During the placement, some performance constraints including the upper limit on assay completion time and maximum allowable chip array should be satisfied, in order that the system reliability and integrity inherent from the architectural-level synthesis can be well-maintained.

Besides, since the increasing assay density and area of DMFBs may potentially reduce yield, a critical issue of *fault tolerance* is also considered to avoid defective cells due to fabrication. Since we need time to ramp up the yield of DMFBs, it is desirable to perform a bioassay on a DMFB with the existence of defects. How to integrate the defect tolerant issue into the placement problem with correct fluidic functions has become an important issue. To handle such a problem, some algorithms, such as SA-based optimization [7], [28] and T-tree-based placement formulation [29], are presented in recent years.

2) Droplet Routing. Droplet routing on DMFBs is a key design issue in the physical-level synthesis, which schedules the movement of each droplet in a time-multiplexed manner. The major goal of droplet routing is constructing the connections between modules, and between modules and I/O ports (i.e., on-chip reservoirs) within different time intervals. This physical synthesis is one of the most critical design challenges due to design complexity as well as large impacts on correct assay performance. Since a microfluidic array is reconfigured dynamically at run-time, the inherent reconfigurability allows different droplet routes to share cells on the micorfluidic array during different time intervals. Besides, a series of 2D placement configurations of fluidic modules in different time intervals are obtained in the placement stage. Therefore, the droplet routing is decomposed into a series of *sub-problems*, which establishes the connections for pre-placed fluidic modules between successive sub-problems. We can thus obtain a complete droplet routing solution by solving these sub-problems sequentially. In this sense, the routes on the microfluidic array can be viewed as *virtual routes* in a three-dimension (3D) manner, which make the droplet routing problem different from the classical wire routing in VLSI designs [30].

During droplet routing, a minimum spacing between different droplets must be maintained to prevent accidental mixing, except for the case when droplet merging is desired (e.g., mixing operation). To realize this feature, *fludic constraints* are introduced to restrict the spacing between droplet routes so as to avoid unexpected mixing [30]. Additionally, the activate modules during droplet routing are treated as obstacles to avoid unexpected mixing. Another constraint in droplet routing is given by a maximum available droplet-routing time. That is, the delay time for each droplet route should not exceed an upper limit (e.g., 10% of the execution time used in scheduling), in order that the system reliability and integrity can be maintained.

The major objective of droplet routing is to minimize the routing length, which is measured by the number of used cells on droplet routes. For a fixed-size microfluidic array, minimum routing length leads to the minimization of the total number of used cells, and thus freeing up more spare cells for better fault tolerance.

Although many state-of-the-art solutions for droplet routing problem have been proposed [30], [31], [32], [33], [34], *cross-*

contamination problem between different droplets has been reported as a weakness of current design automations [33], [35], [36], [37]. During the droplet transportation, molecules and substances carried in droplets may potentially leave traces on the microfluidic array, which causes the contamination problem. The problem occurs more frequently in many protein assays, since proteins tend to adsorb the hydrophobic surface and contaminate it [36], [38]. The particles and liquid residues left behind the microfluidic array potentially lead to an erroneous assay outcome. Moreover, the contaminations left between two adjacent electrodes may cause electrode short problems, which result in physical defects and produce incorrect behaviors in the electrical domain. Although a filler medium, such as silicone oil, has been advocated to prevent contaminations, it has been proved that it is not sufficient for many types of proteins and heterogeneous immunoassays [38].

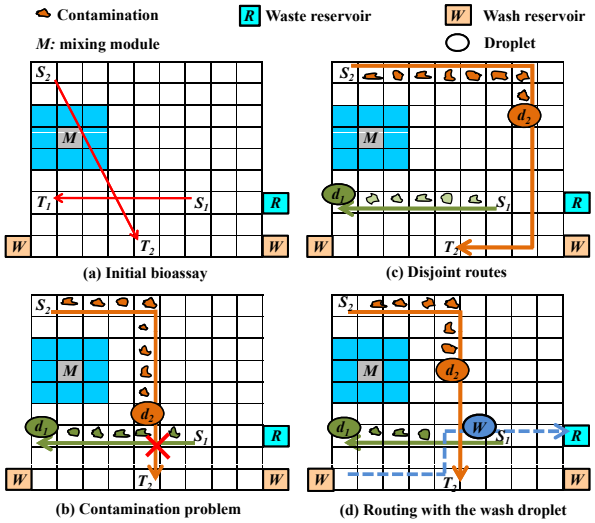

Figure 4. Illustration of the contamination aware droplet routing [39]. (a) Initial bioassay. (b) Cross-contamination problem. (c) Disjoint routing for contamination avoidance. (d) Wash-droplet routing.

For example, let us consider an initial bioassay with two droplets d_1 and d_2, a mixer, and peripheral devices (i.e., reservoirs) as shown in Figure 4(a). The cross-contamination problem occurs when different droplets pass through the same cell, as show in Figure 4(b). Intuitively, contaminations can be avoided by routing in a disjoint manner. This method avoids the overlap between different droplet routes thereby minimizing the likelihood of the contamination problem, as shown in Figure 4(c). However, as the increased design complexity allows more and more biological operations to be performed on a DMFB, finding disjoint routes has become more and more difficult. To cope with this issue, a wash droplet is introduced to clean the contaminated spots on the surface of the microfluidic array, as shown in Figure 4(d). That is, before sharing the routing path, a wash droplet must be routed to clean the contaminations left by the previous droplet. In this regard, how to correctly schedule the wash operations without contamination problem is also a practical concern in the droplet routing problem.

4. Chip-Level Design

Although the fluidic-level synthesis has raised active discussions recently, the chip-level design (i.e., electrical connection) has still not well-studied in current design automations. Unfortunately, the chip-level design, including the *control-pin assignment* and *wire routing*, has been reported as a significant bottleneck in the fabrication of DMFBs [2], [40], [41], [42]. Due to the specialized electrode structure and control mechanism, it is desirable to develop a dedicated automation to assist in the chip-level design of DMFBs. In this section, we introduce the EWOD-chip based microfluidic actuator and the related interconnect problem.

4.1. EWOD-Chip Based Microfluidic Actuator

In performing various fluidic-handling functions, a primary issue is the manipulation of droplets. Although droplets can be controlled on many driving platforms [16], the EWOD chips, also referred to as EWOD actuators, have received much more attention due to their high accuracy and efficiency, and simple fabrication [40]. The EWOD chip generates electric potential by actuating electrodes to change the wettability of droplets, such that droplets can be shaped and driven along the active electrodes [3], [4]. This chip enables the electrical manipulation of droplets with low power consumption, flexibility, and efficiency. Furthermore, their capability of automatic and parallel controls offers faster and more precise execution.

The general diagram of a 2D EWOD chip contains a patterned electrode array, conduction wires, electrical pads, and a substrate [2], [4], [40]. Through these electrical devices, external control circuits can drive these electrodes by assigning time-varying actuation voltage. Thus, by generating electrohydrodynamic force from electrodes, many fluidic-level controls can be performed due to the electrowetting phenomenon [3].

4.2. Electrode Addressing and Routing

To correctly drive the electrodes, *electrode addressing* is introduced as a method through which electrodes are assigned or controlled by pins to identify input signals. Early EWOD-chip designs relied on *direct addressing* [40], where each electrode is directly and independently assigned by a dedicated control pin. This addressing maximizes the flexibility of electrode controls. However, for large arrays, the high pin-count demand complicates the electrical connections, thus rendering this kind of chip unreliable and prohibitively expensive to manufacture [41], [42].

Recently, *pin-constrained* design has been raised as a possible solution to this problem. One of the major approaches, *broadcast addressing*, reduces the number of control pins by assigning a single control pin to multiple electrodes with mutually compatible control signals [42]. In other words, multiple electrodes are controlled by a single control signal and are thus driven simultaneously. In this regard, much ongoing effort has been made to group sets of electrodes that can be driven uniformly without introducing signal conflict [41], [43].

For electrical connections, conduction wires must be routed from the topside electrode array, through the underlying substrate, to the surrounding pads. Hence, after the electrodes are addressed with control pins, the routing problem for EWOD chips can be specified to a 2D pin array, while establishing correspondence between control pins and pads. However, this routing issue is still not well-studied among automations for EWOD chips, revealing an insufficiency of current DMFB design tools. Due to the specialized electrode structure and control mechanism, it is desirable to develop a dedicated routing algorithm for EWOD chips, especially given the issue of the pin-constrained design.

Nevertheless, current chip-level automations are only focus on electrode-addressing manners for control-pin minimization [41], [42], [43], [44], [45], while leaving the interconnect routing as other design consideration. Unfortunately, if routing is simply adopted to an electrode-addressing result, the feasibility and quality of routing solutions may inevitably be limited. For example, Figure 5 illustrates two routing solutions under two different design methods that perform the same fluidic controls. In Figure 5(a), the separate consideration of

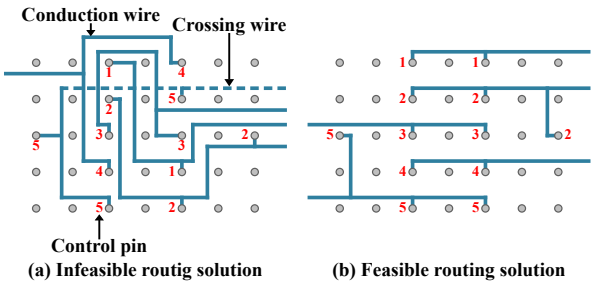

Figure 5. Comparison of two different design methods for performing the same fluidic controls [46]. (a) Considers electrode addressing and routing separately. (b) Considers electrode addressing and routing simultaneously.

electrode addressing and routing results in many back detours for pins 3-4, and thus blocks the routing for pin 5. On the other hand, in Figure 5(b), simultaneous consideration of electrode addressing and routing provides a higher feasibility and quality routing solution in terms of routability and wirelength. In the case of Figure 5(a), additional post processes such as electrode readdressing and rerouting should be further included, and thus the effectiveness of the entire design may be quite restricted. Given these concerns, a novel network-flow based routing algorithm is recently proposed to handle the electrode addressing and routing in a simultaneous manner [46].

5. Testing and Fault Models

In this section, we describe recent advances in the testing of digital microfluidic biochips and fault localization techniques.

5.1. Fault Modeling

As in microelectronic circuits, a defective DMFB is said to have a failure if its operation does not match its specified behavior. In order to facilitate the detection of defects, fault models that efficiently represent the effect of physical defects at some level of abstraction are required. Faults in digital microfluidic systems can be classified as being either catastrophic or parametric. Catastrophic faults lead to a complete malfunction of the system, while parametric faults cause degradation in the system performance. A parametric fault is detectable only if this deviation exceeds the tolerance in system performance.

Table I lists some common failure sources, defects and the corresponding fault models for catastrophic faults in DMFB. Examples of some common parametric faults include the following:

- Geometrical parameter deviation: The deviation in insulator thickness, electrode length and height between parallel plates may exceed their tolerance value.
- Change in viscosity of droplet and filler medium. These can occur during operation due to an unexpected biochemical reaction, or changes in operational environment, e.g., temperature variation.

5.2. Structure Test Techniques

A unified test methodology for DMBF has been presented, whereby faults can be detected by controlling and tracking droplet motion electrically [47]. Test stimuli droplets containing a conductive fluid (e.g., KCL solution) are dispensed from the droplet source. These droplets are guided through the unit cells following the test plan towards the droplet sink, which is connected to an integrated capacitive detection circuit. Most catastrophic faults result in a complete cessation of droplet transportation. Therefore, we can determine the fault-free or faulty status of the system by simply observing the arrival of test stimuli droplets at selected ports. An efficient test plan ensures that testing does not conflict with the normal bioassay, and it guides test stimuli droplets to cover all the unit cells available for testing. The microfluidic array can be modeled as an undirected graph, and the pathway for the test droplet can be determined by solving the Hamiltonian path problem [48]. With negligible hardware overhead, this method also offers an opportunity to implement self-test for microfluidic systems and therefore eliminate the need for costly, bulky, and expensive external test equipment. Furthermore, after detection, droplet flow paths for bioassays can be reconfigured dynamically such that faulty unit cells are bypassed without interrupting the normal operation.

Even though most catastrophic faults lead to a complete cessation of droplet transportation, there exist differences between their corresponding erroneous behaviors. For instance, to test for the electrode-open fault, it is sufficient to move a test droplet from any adjacent cell to the faulty cell. The droplet will always be stuck during its motion due to the failure in charging the control electrode. On the other hand, if we move a test droplet across the faulty cells affected by an electrode-short fault, the test droplet may or may not be stuck depending on its flow direction. Therefore, to detect such faults, it is not enough to solve only the Hamiltonian path problem. In [49], a solution based on Euler paths in graphs is described for detecting electrode shorts.

Despite its effectiveness for detecting electrode shorts, testing based on an Euler path suffers from long test application time. This approach uses only one droplet to traverse the microfluidic array, irrespectively of the array size. Fault diagnosis is carried out by using multiple test application steps and adaptive Euler paths. Such a diagnosis method is inefficient since defect-free cells are tested multiple times. Moreover, the test method leads to a test plan that is specific to a target biochip. If the array dimensions are changed, the test plan must be completely altered. In addition, to facilitate chip testing in the field, test plans need to be programmed into a microcontroller. However, the hardware implementations of test plans from [47] are expensive, especially for low cost, disposable biochips. More recently, a cost-effective testing methodology referred to as "parallel scan-like test" has been proposed [50]. The method is named thus because it manipulates multiple test droplets in parallel to traverse the target microfluidic array, just as test stimuli can be applied in parallel to the different scan chains in an integrated circuit.

A drawback of the above "structural" test methods is that they focus only on physical defects, and they overlook module functionality. Therefore, these methods can only guarantee that a biochip is defect-free. However, a defect-free microfluidic array can also malfunction in many ways. For example, a defect-free reservoir may result in large volume variations when droplets are dispensed from it. A splitter composed of three defect-free electrodes may split a big droplet into two droplets with significantly unbalanced volumes. These phenomena, referred to as malfunctions, are not the result of electrode defects. Instead, they are activated only for certain patterns of droplet movement or fluidic operations. Such malfunctions can have serious consequences on the integrity of bioassay results.

5.3. Functional Test Techniques

Functional testing involves test procedures to check whether groups of cells can be used to perform certain operations, e.g., droplet mixing and splitting. For the test of a specific operation, the corresponding patterns of droplet movement are carried out on the target cluster of cells. If a target cell cluster fails the test, e.g., the mixing test, we label it as a malfunctioning cluster. As in the case of structural testing, fault models must be developed for functional testing.

TABLE I: EXAMPLES OF FAULT MODELS FOR DIGITAL MICROFLUIDIC BIOCHIP

Cause of defect	Defect type	Number of cells	Fault model	Observable error
Excessive actuation voltage applied to an electrode	Dielectric breakdown	1	Droplet-electrode short (a short between the droplet and the electrode)	Droplet undergoes electrolysis, which prevents its further transportation
Electrode actuation for excessive duration	Irreversible charge concentration on an electrode	1	Electrode-stuck-on (the electrode remains constantly activated)	Unintentional droplet operations or stuck droplets
Excessive mechanical force applied to the chip	Misalignment of parallel plates (electrodes and ground plane)	1	Pressure gradient (net static pressure in some direction)	Droplet transportation without activation voltage
Coating failure	Non-uniform dielectric layer	1	Dielectric islands (islands of Teflon coating)	Fragmentation of droplets and their motion is prevented
Abnormal metal layer deposition and etch variation during fabrication	Grounding Failure	1	Floating droplets (droplet are not anchored)	Failure of droplet transportation
	Broken wire to control source	1	Electrode open (electrode actuation is not possible)	Failure to activate the electrode for droplet transportation
	Metal connection between two adjacent electrodes	2	Electrode short (short between electrodes)	A droplet resides in the middle of the two shorted electrodes, and its transport along one or more directions cannot be achieved
Particle contamination or liquid residue	A particle that connect two adjacent electrodes	2	Electrode short	
Protein adsorption during bioassay [10]	Sample residue on electrode surface	1	Resistive open at electrode	Droplet transportation is impeded.
			Contamination	Assay results are outside the range of possible outcomes

Malfunctions in fluidic operations are identified and included in the list of faults; see Table II.

Functional test methods to detect the defects and malfunctions have recently been developed. In particular, dispensing test, mixing test, splitting test, and capacitive sensing test have been described in [51] to address the corresponding malfunctions.

Functional test methods were applied to a PCB microfluidic platform for the Polymerase Chain Reaction (PCR). The platform consists of two columns and two rows of electrodes, three reservoirs, and routing electrodes that connect the reservoirs to the array. An illustration of the mixing and splitting test is shown in Figure 6. The bottom row was first targeted and five test droplets were dispensed to the odd electrodes, as shown in Figure 6(a). Next, splitting test for the even electrodes was carried out. Droplets were split and merged on the even electrodes. In Figure 6(b), we see a series of droplets of the same volume resting on the even electrodes, which means that all the odd electrodes passed the splitting test, and merging at the even electrodes worked well. However, when the splitting test was carried out on the even electrodes, a large variation in droplet volume was observed on the 3rd and 5th electrodes; see Figure 6(c). This variation implied a malfunction, leading to unbalanced splitting on the 4th electrode. The malfunction was detected when the droplets were routed to the capacitive sensing circuit. The 4th electrode on the bottom row was marked as an unqualified splitting site.

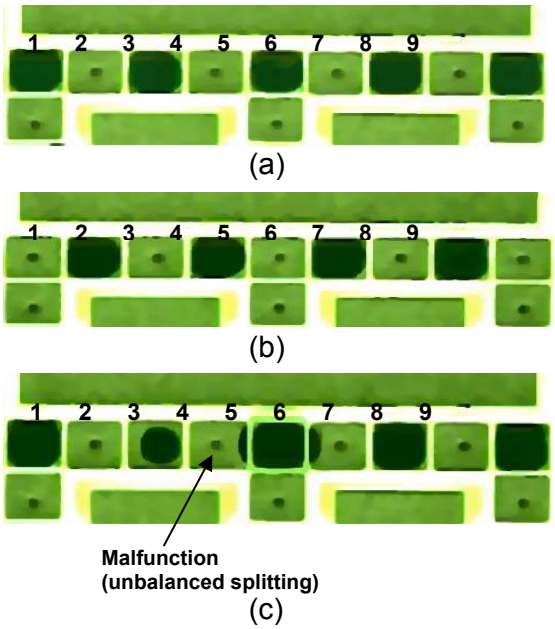

Figure 6. Mixing and splitting test for a fabricated PCR chip.

6. Conclusion

In this paper, we have presented a research survey on design tools for DMFBs. We first provided an overview of the DMFB platform, and highlight emerging applications. Advances in modeling, simulation, fluidic-level synthesis, and chip-level design have been described. Testing and fault model have also been presented. These design techniques are expected to pave the way for the deployment and use of biochips in the emerging marketplace.

7. Acknowledgements

This work was supported in part by the National Science Council of Taiwan ROC under Grant No. NSC 98-2220-E-006-013 and in part by the US National Science Foundation under grant no. CCF-0914895.

References

[1] F. Su and K. Chakrabarty, "Reconfiguration techniques for digital microfluidic biochips," *IEEE DTIP*, pp. 143–148, 2005.

TABLE II: FUNCTIONAL FAULT MODELS

Cause of malfunction	Malfunction type	Number of cells	Fault model	Observable error
Electrode actuation for excessive duration	Irreversible charge concentration on the dispensing electrode	3	Dispensing-stuck-on (droplet is dispensed by not fully cut off from the reservoir)	No droplet can be dispensed from the reservoir
Electrode shape variation in fabrication	Deformity of electrodes	3	No overlap between droplets to be mixed and center electrode	Mixing failure
Electrode electrostatic property variation in fabrication	Unequal actuation voltages	3	Pressure gradient (net static pressure in some direction)	Unbalanced volumes of split droplets
Bad soldering	Parasitic capacitance in the capacitive sensing circuit	1	Oversensitive or insensitive capacitive sensing	False positive/negative in detection

[2] F. Su, K. Chakrabarty, and R. B. Fair, "Microfluidics based biochips: Technology issues, implementation platforms, and design-automation challenges," *IEEE TCAD*, vol. 25, no. 2, pp. 211–223, Feb. 2006.

[3] M. G. Pollack, A. D. Shenderov, and R. B. Fair, "Electrowetting-based actuation of droplets for integrated microfluidics," *LOC*, pp. 96–101, 2002.

[4] J. H. Song, R. Evans, Y. Y. Lin, B. N. Hsu, and R. B. Fair,"A scaling model for electrowetting-on-dielectric microfluidic actuators," *Microfluidics and Nanofluidics*, pp. 75–89, 2009.

[5] T.-W. Huang, S.-Y. Yeh, and T.-Y. Ho, "A network- flow based pin-count aware routing algorithm for broadcast electrode-addressing EWOD chips," *IEEE/ACM ICCAD*, 2010.

[6] F. Su and K. Chakrabarty, "Architectural-level synthesis of digital microfluidics-based biochips," *Proc. IEEE/ACM ICCAD*, pp. 223–228, 2004.

[7] F. Su and K. Chakrabarty, "Unified high-level synthesis and module placement for defect-tolerant microfluidic biochips," *IEEE/ACM DAC*, pp. 825–830, 2005.

[8] K. Chakrabarty, R. B. Fair, and J. Zeng, "Design tools for digital microfluidic biochips: towards functional diversification and more than Moore," *IEEE TCAD*, vol. 29, no. 7, pp. 1001–1017, 2010.

[9] G. Hu and D. Li, "Multiscale phenomena in microfluidics and nanofluidics", *Chemical Engineering Science*, vol. 62, pp. 3443–3454, 2007.

[10] L. G. Leal, *Laminar Flow and Convective Transport Processes: Scaling Principles and Asymptotic Analysis*, Butterworth-Heinemann, 1992.

[11] A. W. Adamson and A. P. Gast, *Physical Chemistry of Surfaces*, Wiley New York, 1997.

[12] A. A. Darhuber, J. P. Valention, S. M. Troian and S. Wagner, "Thermocapillary actuation of droplets on chemically patterned surfaces by programmable microheater arrays", *IEEE J. MEMS*, vol. 12, pp. 873–879, 2003.

[13] K. T. Katz, K. A. Noble and G. W. Faris, "Optical microfluidics", *APL*, vol. 85, no. 13, pp. 2658–2660, 2004.

[14] P. Garstecki, M. J. Fuerstman, H. A. Stone and G. M. Whitesides, "Formation of droplets and bubbles in a microfluidic T-junction - scaling and mechanism of breakup", *LOC*, vol. 6, pp. 437–446, 2006.

[15] U. Lehmann, S. Hadjidj, V. K. Parashar, A. Rida and M. A. M. Gijs, "Two dimensional magnetic manipulation of microdroplets on a chip", *Transducers*, 2005.

[16] J. A. Schwartz, J. V. Vykoukal and P. R. C. Gascoyne, "Droplet-based chemistry on a programmable micro-chip", *LOC*, vol. 4, pp. 11–17, 2004.

[17] M. G. Pollack, R. B. Fair and A. D. Shenderov, "Electrowetting based actuation of liquid droplets for microfluidic applications", *APL*, vol. 77, no. 11, pp. 1725, 2000.

[18] R. Sista, Z. Hua, P. Thwar, A. Sudarsan, V. Srinivasan, A. Eckhardt, M. Pollack and V. Pamula, "Development of a digital microfluidic platform for point of care testing", *LOC*, vol. 8, pp. 2091–2104, 2008.

[19] F. H. Harlow and J. E. Welch, "Numerical study of large amplitude free surface motions", *Physics of Fluids*, vol. 9, pp. 842–851, 1966.

[20] C. W. Hirt and B. D. Nichols, "Volume of Fluid (VOF) method for the dynamics of free boundaries", *Journal of Computational Physics*, vol. 39, pp. 201–225, 1981.

[21] J. A. Sethian, *Level Set Methods and Fast Marching Methods: Evolving Interfaces in Computational Geometry, Fluid Mechanics, Computer Vision, and Materials Science*, Cambridge University Press, 1999.

[22] S. O. Unverdi and G. Tryggvason, "A front-tracking method for viscous, incompressible, multi-fluid flows", *Journal of Computational Physics*, vol. 100, pp. 25–37, 1992.

[23] X. W. Shan and H. D. Chen, "Lattice Boltzmann model for simulation flows with multiple phases and components", *Physics Review E*, vol. 47, pp. 1815–1819, 1993.

[24] J. Zeng, "Modeling and simulation of electrified droplets and its application to computer-aided design of digital microfluidics", *IEEE TCAD*, vol. 25, no. 2, pp. 224–233, 2006.

[25] E. Maftei, P. Paul, and J. Madsen, "Tabu search-based synthesis of dynamically reconfigurable digital microfluidic biochips" , *ACM CASES*, pp. 195–203, 2009.

[26] F. Su and K. Chakrabarty, "Architectural-level synthesis of digital microfluidics-based biochips," *IEEE/ACM ICCAD*, pp. 223–228, 2004.

[27] Y. Zhao, T. Xu and K. Chakrabarty, "Control-path design and error recovery in digital microfluidic lab-on-chip," *ACM JETC*, vol. 3, No. 11, 2010.

[28] F. Su and K. Chakrabarty, "Module placement for fault-tolerant microfluidics-based biochips," *ACM TODAES*, vol. 11, pp. 682–710, 2006.

[29] P.-H. Yuh, C.-L. Yang, and Y.-W. Chang, "Placement of defect-tolerant digital microfluidic biochips using the T-tree formulation," *ACM JETC*, vol. 3, no. 3, 2007.

[30] F. Su, W. Hwang, and K. Chakrabarty, "Droplet routing in the synthesis of digital microfluidic biochips," *IEEE/ACM DATE*, pp. 1–6, 2006.

[31] K. F. B$^{'}$ohringer, "Modeling and controlling parallel tasks in droplet based microfluidic systems," *IEEE TCAD*, vol. 25, no. 2, pp. 334–344, 2006.

[32] M. Cho and D. Z. Pan, "A high-performance droplet routing algorithm for digital microfluidic biochips," *IEEE TCAD*, vol. 27, no. 10, pp. 1714–1724, 2008.

[33] T.-W. Huang and T.-Y. Ho, "A fast routability- and performance-driven droplet routing algorithm for digital microfluidic biochips," *IEEE ICCD*, pp. 445–450, 2009.

[34] P.-H. Yuh, C.-L. Yang, and Y.-W. Chang, "BioRoute: A network flow based routing algorithm for the synthesis of digital microfluidic biochips," *IEEE TCAD*, vol. 27, no. 11, pp. 1928–1941, 2008.

[35] C. C.-Y. Lin and Y.-W. Chang, "Cross-contamination aware design methodology for pin-constrained digital microfluidic biochips," *IEEE/ACM DAC*, pp. 641–646, 2010.

[36] Y. Zhao and K. Chakrabarty, "Cross-contamination avoidance for droplet routing in digital micro fluidic biochips," *IEEE/ACM DATE*, pp. 1290–1295, 2009.

[37] Y. Zhao and K. Chakrabarty, "Synchronization of washing operations with droplet routing for cross-contamination avoidance in digital microfluidic biochips," *IEEE/ACM DAC*, pp.635–640, 2010.

[38] J. Y. Toon and R. L. Garrell, "Preventing biomolecular adsorption in electrowetting-based biofluidic chips, " *Anal. Chem.*, vol. 75, no. 19, pp. 5097–5102, 2003.

[39] T.-W. Huang, C.-H. Lin, and T.-Y. Ho, "A contamination aware droplet routing algorithm for digital microfluidic biochips," *IEEE/ACM ICCAD*, pp. 151–156, 2009.

[40] J. Gong and C. J. Kim, "Direct-referencing two-dimensional-array digital microfluidics using multilayer printed circuit board," *IEEE J. MEMS*, no. 2, pp. 257–264, 2008.

[41] T. Xu, K. Chakrabarty and V. K. Pamula, "Defect-tolerant design and optimization of a digital microfluidic biochip for protein crystallization," *IEEE TCAD*, vol. 29, pp. 552–565, 2010.

[42] T. Xu and K. Chakrabarty, "Broadcast electrode-addressing for pin-constrained multi-functional digital microfluidic biochips," *IEEE/ACM DAC*, pp. 173–178, 2008.

[43] T. Xu and K. Chakrabarty, "Droplet-trace-based array partitioning and a pin assignment algorithm for the automated design of digital microfluidic biochips," *IEEE/ACM CODES+ISSS*, pp. 112–117, 2006.

[44] T.-W. Huang and T.-Y. Ho, "A two-stage ILP-based droplet routing algorithm for pin-constrained digital microfluidic biochips," *ACM ISPD*, pp. 201–208, 2010.

[45] C. C.-Y. Lin and Y.-W. Chang, "ILP-based pin-count aware design methodology for microfluidic biochips," *IEEE TCAD*, 2010.

[46] T.-W. Huang, S.-Y. Yeh, and T.-Y. Ho, "A network-flow based pin-count aware routing algorithm for broadcast electrode-addressing EWOD chips," *IEEE/ACM ICCAD*, 2010.

[47] F. Su, S. Ozev and K. Chakrabarty, "Ensuring the operational health of droplet-based microelectrofluidic biosensor systems", *IEEE Sensors*, vol. 5, pp. 763–773, 2005.

[48] F. Su, S. Ozev and K. Chakrabarty, "Test planning and test resource optimization for droplet-based microfluidic systems", *JETTA*, vol. 22, pp. 199–210, 2006.

[49] F. Su, W. Hwang, A. Mukherjee and K. Chakrabarty, "Testing and diagnosis of realistic defects in digital microfluidic biochips", *JETTA*, vol. 23, pp. 219–233, 2007.

[50] T. Xu and K. Chakrabarty, "Parallel scan-like test and multiple-defect diagnosis for digital microfluidic biochips", *IEEE Trans. BioCAS*, vol. 1, pp. 148–158, 2007.

[51] T. Xu and K. Chakrabarty, "Functional testing of digital microfluidic biochips", *IEEE ITC*, 2007.